Radiotherapy and Oncology 141 (2019) 214–219

Contents lists available at ScienceDirect

Radiotherapy and Oncology

journal homepage: www.thegreenjournal.com

Original Article

[^{68}Ga-]PSMA-11 PET/CT and multiparametric MRI for gross tumor volume delineation in a slice by slice analysis with whole mount histopathology as a reference standard – Implications for focal radiotherapy planning in primary prostate cancer

Alisa S. Bettermann [a,*,1], Constantinos Zamboglou [a,g,h,1], Selina Kiefer [b], Cordula A. Jilg [c], Simon Spohn [a,g], Jasmin Kranz-Rudolph [a,g], Thomas F. Fassbender [d], Peter Bronsert [b,g], Nils H. Nicolay [a,g], Christian Gratzke [c], Michael Bock [e], Juri Ruf [d], Matthias Benndorf [f,1], Anca L. Grosu [a,g,1]

[a] Department of Radiation Oncology; [b] Institute for Surgical Pathology; [c] Department of Urology; [d] Department of Nuclear Medicine; [e] Department of Radiology, Division of Medical Physics; [f] Department of Radiology, Medical Center – University of Freiburg, Faculty of Medicine, University of Freiburg; [g] German Cancer Consortium (DKTK), Partner Site Freiburg; and [h] Berta-Ottenstein-Programme, Faculty of Medicine, University of Freiburg, Germany

ARTICLE INFO

Article history:
Received 22 May 2019
Received in revised form 3 July 2019
Accepted 3 July 2019
Available online 17 August 2019

Keywords:
Prostate cancer
PSMA-PET
MpMRI
Histopathology
Focal therapy

ABSTRACT

Background and purpose: Focal therapies are a promising approach to treat prostate cancer (PCa) more precisely instead of conventional whole gland treatment. Nowadays, multiparametric MRI (mpMRI) is routinely used for gross tumor volume (GTV) delineation. The aim of our study was to compare PSMA-PET/CT and mpMRI for the delineation of intraprostatic tumor burden by using whole mount histopathology as a reference standard.

Material and methods: 17 prospectively enrolled patients with primary PCa underwent [^{68}Ga-]PSMA-11 PET/CT and mpMRI before radical prostatectomy. PSMA-PET/CT, mpMRI and histopathology of the resected specimens were co-registered. Two teams of experts generated GTV contours for mpMRI and PET, respectively. The imaging was validated on a lesion level and slice by slice in quadrants based on the distribution of PCa in histopathology. Overall, 772 quadrants were analyzed with 414 being true positive for tumor (53.6%).

Results: Median tumor volumes were 10.4 ml for GTV-histo, 10.8 ml for PSMA-PET and 4.5 ml for mpMRI. Median tumor volume in mpMRI was significant ($p < 0.05$) smaller than GTV-PET and GTV-histo, respectively. The sensitivity and specificity were 86% and 87% for PSMA-PET, 58% and 94% for mpMRI and 91% and 84% for their GTV-union. In 133 quadrants PSMA-PET/CT correctly identified tumor where mpMRI found none. MpMRI identified 19 true positive quadrants exclusively.

Conclusion: Our investigation demonstrates an increased consensus of PSMA-PET with histopathology compared to mpMRI for intraprostatic GTV delineation, especially with a higher sensitivity. Additionally mpMRI contours underestimate tumor volume significantly. Thus PSMA-PET may be a complementary augmentation for GTV delineation in focal therapies.

Conventionally the whole prostate is irradiated with a homogeneous dose to the entire gland in patients with primary prostate cancer (PCa) [1]. Even though an escalation of radiation dose is known to benefit tumor response, escalation to the whole prostate is not feasible due to toxicity [2,3]. This can lead to pivotal lesions lacking a proper dose and response [4]. For this reason local recurrences often arise at the primary location of malignant lesions [4,5]. The concept of focal therapies in PCa was implemented to tackle this challenge and is currently subject to extensive research (e.g. the FLAME trail (NCT01168479) and the PIVOTALBoost trial) [6,7]. In an era of high-precision radiotherapy this strategy relies on a sensitive detection of significant malignant lesions and their extension to allow proper patient selection and optimal treatment. At present, mpMRI is the gold standard for staging and gross tumor volume (GTV) delineation for radiotherapy treatment planning in PCa. However, it is limited by a complex interpretation with pitfalls and may underestimate the true tumor mass [8–10]. As intraprostatic GTV delineation remains controversial in mpMRI, the implementation of alternative diagnostic imaging approaches is warranted. Prostate Specific Membrane Antigen (PSMA) has been

* Corresponding author.
[1] Contributed equally.

https://doi.org/10.1016/j.radonc.2019.07.005
0167-8140/

found to be selectively overexpressed in PCa cells and can be traced by radio-labelled peptide ligands, e.g. [^{68}Ga-]PSMA-11 in positron emission tomography (PET) [11]. PSMA-PET/CT is already on the verge of being established as the gold standard for restaging in recurrent PCa after surgery [12,13]. However, its potential to guide therapies in a first line diagnostic setting needs to be investigated more thoroughly. Concordantly to others, our group already postulated the superiority of PSMA-PET [14]. The aim of this study is to compare the performance of mpMRI and PSMA-PET/CT in intraprostatic GTV delineation on a slice by slice- and lesion-level using co-registered whole mount histopathology after surgery as the standard of reference and to discuss the consequences for focal radiation therapy.

Methods

Study design and patient population

In this study 20 patients were prospectively enrolled with histopathologically proven primary adenocarcinoma of the prostate and a [^{68}Ga-]PSMA-11 PET/CT scan before prostatectomy. Exclusion criteria were a previous transurethral resection of the prostate and neoadjuvant deprivation therapy. Three patients were excluded in the current analysis because mpMRI was not mandatory in the study protocol and only performed in 17 patients. The median time difference between PSMA-PET/CT and mpMRI scan was 35 days (range: 0–199 days). The median age was 67 years and the median PSA was 17.4 (ng/ml). Informed written consent was obtained from all patients and the ethics committee approved this study. An interim analysis of seven patients had already been published by our group [14]. Further information on the patients and their respective characteristics is given in Table 1.

PSMA-PET/CT

The protocol of the radiolabeling of [^{68}Ga-]PSMA-11 has been previously described in Zamboglou et al. [15]. A whole body PSMA-PET/CT scan was performed one hour after the injection of the radiotracer. Three different Philips scanners were used in this study: GEMINI TF TOF 64 (8 Patients), GEMINI TF 16 Big Bore (6 Patients) and Vereos (3 Patients). All scanners attained the requirements of the imaging guidelines proposed by the European Association of Nuclear Medicine (EANM) and acquired EANM Research Ltd. (EARL) accreditation during acquisition. Images were modified to decay corrected injected activity per kg body weight (SUV [g/ml]). Two experienced nuclear physicians delineated the GTV in consensus (GTV-PET) under blind conditions in iPLAN (RT image 4.7.7; BrainLAB, Germany). The minimum and maximum voxel values were set from 0 to 5 SUV. The presence of PCa on PET images was defined as mono- or multifocal uptake greater than adjacent background in more than one slice. Anatomical orientation was provided by the CT scans. The prostate volume on CT was delineated by an experienced reader.

MpMRI

Multiparametric MRI of the prostate was performed at 3 Tesla in 13 Patients (10 patients were examined with a TrioTim, Siemens Germany, 2 patients were examined with a Magnetom Vida, Siemens, Germany, and 1 patient was examined with a Skyra, Siemens, Germany). In 4 patients, mpMRI was performed at 1.5 Tesla (3 patients were examined with an Aera, Siemens, Germany and 1 patient was examined with an Avanto, Siemens, Germany). In all patients, triplanar (axial, coronal, sagittal) T2 weighted turbo spin echo sequences (TE range axial images: 102–119 ms, TR range axial images: 3570–9400 ms, with 5500 ms for all patients at the 3 T Trio Tim) and axial echo planar imaging diffusion weighted imaging (low b-value 0 or 50 s/mm^2 for all patients, high b-value 800 s/mm^2 for 14 patients and 1000 s/mm^2 for 3 patients) was part of the MRI protocol. ADC (apparent diffusion coefficient) maps were calculated for the diffusion weighted sequence. No endorectal coils were employed.

A team of one board-certified radiologist, trained in the interpretation of prostate MRI and one radiation oncologist with experience in the interpretation of prostate MRI, delineated all areas suspicious for significant tumor in the axial T2 weighted sequence in consensus (GTV-MRI). At the time of interpretation, both T2 weighted images and diffusion weighted images (including ADC maps) were available to the readers but they were blinded to the histopathological information. The readers applied standardized imaging criteria (PI-RADSv2, prostate imaging: reporting and data system) to evaluate tumor extent [16]. Lesions with a PI-RADS category $\geq$3 were considered positive. Additionally the prostate volume on T2w-MR images was contoured by an experienced

Table 1
Patient characteristics and GTV-histo: Column 1–5 lists patient characteristics. Please note that the pT, pN and the Gleason score were assigned postoperatively based on the resected prostate und lymph nodes. Patient 1–7 were included in the mentioned previous study [14]. Column 6–7 report GTV-histo and PCa as percentage of prostate tissue. The prostate volume was delineated on CT.

Patient #	Age (years)	PSA (ng/ml)	TNM	Gleason score	GTV-histo (ml)	PCa (% of prostate tissue)
1	67	6.1	pT3a pN0 cM0	3+4 (7a)	11.0	25.9
2	61	10.6	pT2c pN0 cM0	3+4 (7a)	5.6	17.2
3	52	51.1	pT3b pN1 cM0	5+4 (9)	24.5	42.2
4	60	49.0	pT2c pN1 cM0	3+4 (7a)	19.8	28.7
5	73	25.5	pT2c pN0 cM0	3+4 (7a)	2.8	3.9
6	59	9.2	pT2c pN0 cM0	4+3 (7b)	3.2	6.3
7	74	8.8	pT2c pN0 cM0	3+4 (7a)	1.6	2.4
8	74	15.0	pT2c pN0 cM0	3+4 (7a)	2.1	2.7
9	51	17.4	pT3a pN0 cM0	4+3 (7b)	4.2	12.0
10	48	23.0	pT3b pN1 cM0	4+3 (7b)	18.8	44.8
11	76	20.7	pT2c pN0 cM0	4+3 (7b)	9.7	21.6
12	59	15.8	pT3b pN1 cM0	4+5 (9)	15.9	58
13	73	40.0	pT3a pN1 cM0	4+5 (9)	20.5	47.7
14	53	16.3	pT3a pN0 cM0	4+4 (8)	6.7	17.2
15	72	28.9	pT3b pN1 cM0	4+4 (8)	19.9	17.0
16	70	16.0	pT3a pN0 cM0	4+3 (7b)	10.4	9.8
17	67	218.0	pT3b pN0 cM0	4+4 (8)	103.0	59.1
Median	67	17.4		7b	10.4	17.2
Min	48	6.01		7a	1.60	2.4
Max	76	218.0		9	103.0	59.1

reader. The prostate was delineated on MRI and CT (from PSMA PET/CT), because the histology was registered on an ex vivo CT. This might have overestimated GTV-histo at the expense of GTV-MRI. GTV-MRI was adjusted (GTV-MRI-adj) by the divided prostate volume coefficient to match GTV-histo and GTV-PET.

$$GTV - MRI - adj = GTV - MRI * \frac{Volume\ of\ prostate\ CT}{Volume\ of\ prostate\ MRI}$$

Each patient was adjusted individually (Supplementary Table 1).

Pathology

After resection, the prostate was marked with tissue marking dyes and was agarose fixated within a customized localizer. Subsequently, the localizer was scanned in an ex vivo CT. The resected prostate was sliced perpendicularly to the urethra in the same angle as the ex vivo CT by using an in-house cutting device. Consequently, the slices of the ex vivo CT were consonant with histopathological slices. Two experienced pathologists delineated malignant areas on each H&E stained whole-mount slice. These histopathology sections including PCa GTV delineations were digitized and manually matched to the ex vivo CT in MITK (MITK Workbench 2014.10.00). The GTV contours on ex vivo CT slices were automatically interpolated in MITK to obtain GTV-histo (Table 1) [17].

Co-registration

PSMA-PET/CT, mpMRI images and histopathology were co-registered in line with our published in-house protocols [14]. To view the histopathology delineation on the same spatial frame - the in vivo CT from PSMA-PET scans - a spatial correspondence between ex vivo and in vivo CT was established. For this purpose, reproducible anatomic landmarks were verified and a careful non-rigid deformation was performed. After this sub-registration step, the CT, including the segmentations, were imported into Eclipse v15.1 (Varian). Subsequently, the other two imaging modalities PSMA-PET (hardware-based registration) and T2w-MRI (mutual information registration between T2w and CT images) and their contours were automatically aligned onto the in vivo CT in Eclipse (Fig. 1). A manual correction based on anatomic landmarks in the pelvis was performed whenever necessary.

Slice by slice analysis

The analysis was conducted slice by slice and quadrant-based from apex to base (Fig. 1). Sensitivity and specificity was determined for each imaging modality, subsequently GTV-union and GTV-intersection were derived. GTV-union is defined as the merged contours of PSMA-PET and mpMRI. The GTV-intersection is the conjunction of GTV-PET and GTV-MRI. In order to account for errors in image co-registration, only lesions extending more than 3 mm into another quadrant were counted as tumor positive lesions in that quadrant.

Statistical analysis

Statistical analysis was performed with Prism 7 for Windows (GraphPad Software, La Jolla California US) and Microsoft Excel 2010 (Microsoft, Redmond, USA). Pairwise comparison was performed with Wilcoxon test, the threshold for significance was $p < 0.05$.

Results

In a slice-based analysis 193 slices from 17 patients were analyzed (mean 11.4 slices per patient) with a quadrant-based method. Thus, 772 quadrants were evaluated. According to GTV-histo 414 quadrants (53.6%) contained tumor tissue. Taking true positive and negative quadrants into account PSMA-PET diagnosed 668 quadrants (86.5%) correct whilst mpMRI correctly identified 577 (74.7%). By comparing only GTV-histo positive quadrants, 133 quadrants were identified true positive by PSMA-PET/CT in which mpMRI was false negative. In contrast to that, mpMRI exclusively detected GTV-histo in 19 quadrants (Fig. 2).

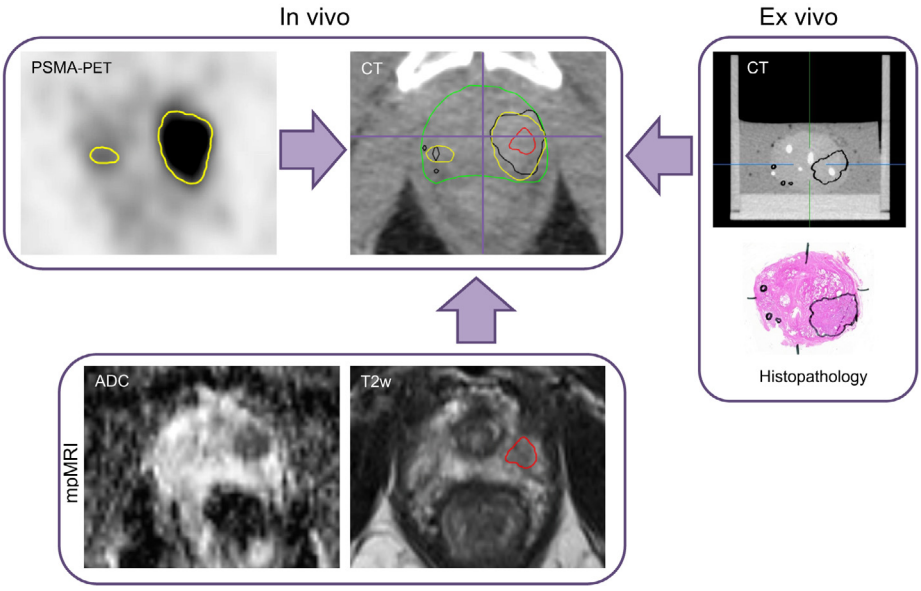

Fig. 1. Co-registration: This figure depicts the co-registration process based on patient 6, a 59 year old patient with a PSA of 9.2 ng/ml. Histopathology demonstrated a Gleason 4+4 tumor in the indicated areas (black). PSMA-PET was registered hardware based to the in vivo CT. Everything else, T2w mpMRI and ex vivo CT, were registered onto the in vivo CT as well. Though histopathology was sub-registered to an ex vivo CT of the resected prostates first. On the in vivo CT GTV-PET is contoured in yellow, GTV-MRI in red and histopathology in black. The prostate (green) was separated into four equal quadrants illustrated in purple.

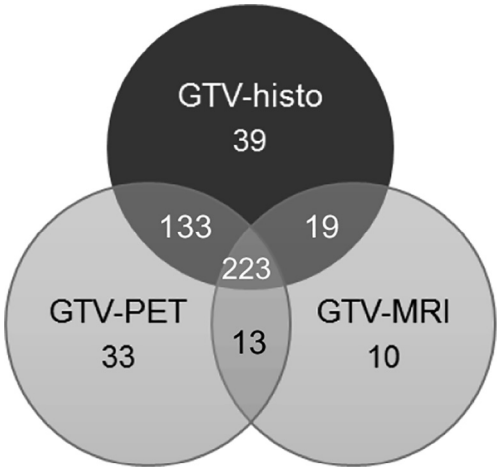

Fig. 2. Venn diagram: Each circle represents the set of tumor positive quadrants of an imaging modality or histopathology. GTV-histo is visualized in black as ground truth. The overlap of tumor positive detection rates of PSMA-PET, mpMRI and histopathology are illustrated. PSMA-PET identified 133 quadrants which were true positive where mpMRI detected none. In contrast, mpMRI alone detected tumor in 19 quadrants in which PSMA-PET was false negative. In 223 quadrants both scans concordantly detected tumor lesions found in histopathology. 13 quadrants were false negative in both modalities. Overall 39 quadrants containing tumor tissue were missed. 33 quadrants in PET and 10 quadrants in MRI were false positive.

The quadrant-based sensitivity and specificity as well as their GTV-union and GTV-intersection were calculated for each modality. The sensitivity and specificity for GTV-PET were 86% and 87% respectively and for mpMRI 58% and 94%. The GTV-union of mpMRI and PSMA-PET/CT achieved the highest sensitivity (91%) and lowest specificity (84%), whereas their intersection had the lowest sensitivity (54%) and highest specificity (96%). The sensitivity and specificity per patient refer to inter-patient variability and are listed in Supplementary Table 2. Once the 4 patients with a 1.5 Tesla scan were excluded the sensitivity for GTV-MRI rose to 61%.

In a lesion-based analysis the median volume of GTV-histo was 10.4 ml (Range: 1.6–103 ml), in PSMA-PET/CT 10.8 ml (range: 0.7–101.4 ml) and in mpMRI 4.5 ml (range: 0.7–58.7 ml). Tumor volume in mpMRI was statistically significant smaller than GTV-histo ($p = 0.0042$) and tumor volume in PET ($p = 0.0052$), respectively. In spite of that, no significant difference was observed between PSMA-PET and GTV-histo ($p = 0.59$) (Fig. 3). The median GTV-MRI-adj was 4.8 ml (range: 0.6–73.8 ml) which was still statistically significant ($p > 0.05$) smaller than GTV-histo (Supplementary Table 1).

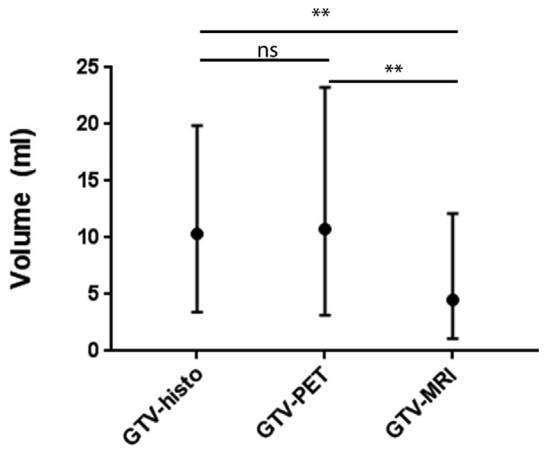

Fig. 3. Significance: This figure depicts the GTV in ml delineated on each imaging modality. Each item and its vertical extension depict the median tumor volume and the interquartile ranges of the respective GTVs. 'ns' is defined as not significant ($p > 0.05$) and "**" as significant ($p < 0.05$).

A total number of 32 lesions were confirmed by the pathologists. Almost every patient had an index lesion defined as the largest tumor focus with a minimum diameter of 5 mm. All of them were spotted in both imaging modalities (besides patient 16). 9 patients had unifocal lesions, ranging from 1.6 ml to 24.5 ml, all being identified on mpMRI as well as PSMA-PET/CT. Multifocal PCa was found in 8 patients of whom one patient (patient 16) had only very small microlesions. This patient had been excluded from lesion analyses because he would not have been considered for focal radiotherapy approaches. The remaining 7 patients had overall 23 lesions (range: 2–7 lesions) in histopathology. PSMA-PET identified 13 lesions while mpMRI found 11. Both scans detected 16 lesions complementary (Table 2).

Discussion

Nowadays, mpMRI is used as a gold standard for primary staging, biopsy guidance and focal radiation therapy planning of primary PCa [1]. Its application is nevertheless controversial for the exact determination of tumor burden. In a recent study Johnson et al. correlated lesions in a 3 T mpMRI with whole mount pathology in 588 patients [10]. The mpMRI identified 65% of clinically significant tumor lesions. In addition, 23% of the solitary and 7% of the multifocal significant lesions being missed had a GS $\geq$4+3 assigned [10]. Incomplete coverage of intraprostatic tumor burden may explain the findings of a recent study by Peters et al. [18]. 30 patients with low to intermediate risk PCa received 19 Gray using High-Dose-Rate Brachytherapy to lesions visible on mpMRI expanded by a 5 mm margin. However, 7/9 patients had intraprostatic recurrences out of the radiation field [18,19]. In direct comparison with mpMRI, PSMA-PET has been proposed as an appropriate alternative for more exact tumor volume delineation in previous studies and the results concur with our investigation (Table 3) [20–25].

In the seven studies of Table 3 the methods used for image processing and interpretation vary widely and yet certain tendencies may be observed. The specificity of PSMA-PET (Range: 0.71–0.95) inclines to be quite similar to the specificity of mpMRI (Range: 0.64–0.94). The sensitivity of PSMA-PET ranges from 0.49 to 0.89 and is in most cases higher than the corresponding sensitivity of mpMRI. Only in the study of Kesch et al. the sensitivity of PSMA-PET is lower than the sensitivity of mpMRI (0.71 vs. 0.86) [23]. In our study, PSMA-PET detected real tumor in 133 more quadrants (17.23%) where mpMRI identified none. On the contrary, all the index lesions were spotted on PSMA-PET and mpMRI, respectively, and both imaging modalities had only a poor (mpMRI) and moderate (PSMA-PET) performance in detection of secondary lesions. Thus, the increased sensitivity of PSMA-PET seems to rely on the detection of tumor volume. The median GTV in histopathology (10.4 ml) was significantly larger than the median delineated volume of malignant lesions in mpMRI (4.5 ml) with a median difference of 5.5 ml. In contrast, no significant ($p > 0.05$) difference was observed between GTV-PET (median: 10.8 ml) and GTV-histo. These findings suggest that the mpMRI underestimates the tumor burden compared to PSMA-PET. Even smaller tumor volumes were contoured in mpMRI by van Schie et al. (median: 0.69–3.6 ml) [26]. An option to improve sensitivity of GTV-MRI might be the adaption of a safety margin in terms of a clinical target volume (CTV). We applied a 3 mm margin in analogy to the PIVOTALBoost trail (Supplementary Table 1) [27]. Sensitivity rose to 80% and GTV-MRI volume to a median of 11.9 ml. But the true CTV expansion

Table 2
Lesion analysis: Lesions were divided in unifocal (n = 9), multifocal (n = 7), index and secondary lesions and the total number is stated at the bottom. The columns list the numbers of lesions detected in histopathology (as a ground truth), mpMRI, PSMA-PET and the union of both. Patient 16 was excluded from lesion analysis due to multifocal microlesions. The index lesion was defined as the largest lesion per patient with a minimum diameter of 5 mm.

Lesions	Histopathology	mpMRI	PSMA-PET	mpMRI+PSMA-PET
Unifocal (9 patients)	9	9	9	9
Multifocal (7 patients)	23	11	13	16
• Index	7	7	7	7
• Secondary	16	4	6	9
In total	32	20	22	25

Table 3
Corresponding studies: This table shows the accuracy determined in 7 different studies comparing PSMA-PET, mpMRI and whole-mount histopathology. It is noteworthy that these studies were performed with various methods.

	PSMA-PET		MRI		GTV-union	
	Sensitivity	Specificity	Sensitivity	Specificity	Sensitivity	Specificity
Our study	0.86	0.87	0.58	0.94	0.91	0.84
Eiber et al. [20]	0.64	0.94	0.43/0.58*	0.82/0.98*	0.76	0.97
Rhee et al. [21]	0.49	0.95	0.44	0.94		
Berger et al. [22]**	0.81	0.85	0.65	0.83		
Kesch et al. [23]†	0.71	0.81	0.86	0.64	0.81	0.81
Chen et al. [24]	0.89	0.71	0.76	0.88	0.89	0.96
Hicks et al. [25]#			0.42	0.79	0.67	0.71

* Eiber et al. used reported two diagnostic values based on Youden-selected thresholds.
** Berger et al. only included index lesion in their analyses.
† Kesch et al. used 18F-PSMA-1007-PET/CT as radiotracer.
# Hicks et al. performed a PSMA-PET/MRI scan. Accuracy was determined on a raw stringent approach meaning that tumor foci were detected in the same region.

required to improve MRI's sensitivity is still unknown and further studies are warranted.

It is vital to consider that conspicuous low sensitivities for GTV-PET were observed in two patients (Patient 7 = 0.14; Patient 16 = 0.27). This may be caused by heterogeneous PSMA expression which has been observed by Mannweiler et al., performing immunostaining [28]. Another explanation might be the low volume of patient 7 (1.6 ml) and the multifocal microlesions of patient 16 (Supplementary Table 1). Also Donato et al. observed that some low volume (0.35 ml and 0.72 ml) and GS 4+3 tumors were not seen on PSMA-PET (n = 2) [29].

Since mpMRI identified tumor burden in 19 additional quadrants exclusively (2.46%), the combined usage of mpMRI and PSMA-PET (GTV-union) further augments sensitivity than PSMA-PET scan alone. Donato et al. reported similar findings regarding the detection of lesions though. 15.9% were solely seen on PSMA-PET while 7.9% were only seen on mpMRI [29]. The combination of PSMA-PET/CT and mpMRI is highlighted by Eiber et al. as well [20]. Our study confirms the recommendation since GTV-union is slight but significant ($p < 0.05$) better than GTV-PET alone. Taken together, the simultaneous usage of PSMA-PET and mpMRI will remain an appropriate method until patients with a low sensitivity on PSMA-PET can be accurately identified by clinical surrogate parameters before imaging.

Our study is limited to a patient cohort undergoing prostatectomy with intermediate- and high-risk PCa according to D'Amico's risk criteria [30]. But especially these patients warrant new treatment modalities due to inadequate treatment outcomes with freedom of biochemical relapse of 60–90% at five years after whole-gland radiotherapy [31–33]. However, low risk patients are also a suitable for ultra-focal therapies as an alternative to active surveillance [18]. The accuracy of PSMA-PET should, therefore, be further evaluated in this patient group. Even though our study only included 17 patients, reporting can be justified by considering the labor-intensive processing required for each patient. Furthermore, the co-registration of whole-mount specimen, PET and mpMRI images only cause minimal misalignment. Ex vivo CT scans from the resected prostates were registered on the in vivo CT of the PSMA-PET/CT, favoring PSMA-PET thereby. This concern was tackled by the application of an established co-registration protocol and a quadrant-based analysis. Additionally, the GTV-MRI-adj was adjusted by the prostate volume coefficient of mpMRI and CT to out rule overestimation of GTV-histo in correspondence to GTV-MRI. Another factor that might be a disadvantage for mpMRI is the use of 1.5 Tesla MRIs on 4 patients and the heterogeneous imaging protocols used for mpMRI acquisition. However, when patients examined in 1.5 Tesla scanners were excluded, mpMRI's sensitivity increased only slightly to 60%.

In conclusion, PSMA-PET showed improved performance for intraprostatic GTV delineation compared to mpMRI based on validation with histopathology as standard of reference. Thus, PSMA-PET could be implemented as an add-on to mpMRI in focal radiotherapy concepts for patients with primary prostate cancer enabling more personalized treatment planning.

Declaration of Competing Interest

All authors declare no conflict of interest.

Appendix A. Supplementary data

Supplementary data to this article can be found online at https://doi.org/10.1016/j.radonc.2019.07.005.

References

[1] Mottet N, Bellmunt J, Bolla M, Briers E, Cumberbatch MG, De Santis M, et al. Guidelines on prostate cancer. Part 1: screening, diagnosis, and local treatment with curative intent. Eur Urol 2017;71:618–29.
[2] Viani GA, Stefano EJ, Afonso SL. Higher-than-conventional radiation doses in localized prostate cancer treatment: a meta-analysis of randomized, Controlled Trials. Int J Radiat Oncol 2009;74:1405–18.
[3] Peeters STH, Heemsbergen WD, Koper PCM, van Putten WLJ, Slot A, Dielwart MFH, et al. Dose-response in radiotherapy for localized prostate cancer: results of the Dutch multicenter randomized phase III trial comparing 68 Gy of radiotherapy With 78 Gy. J Clin Oncol 2006;24:1990–6.

[4] Cellini N, Morganti AG, Mattiucci GC, Valentini V, Leone M, Luzi S, et al. Analysis of intraprostatic failures in patients treated with hormonal therapy and radiotherapy: implications for conformal therapy planning. Int J Radiat Oncol 2002;53:595–9.
[5] Pucar D, Hricak H, Shukla-Dave A, Kuroiwa K, Drobnjak M, Eastham J, et al. Clinically significant prostate cancer local recurrence after radiation therapy occurs at the site of primary tumor: magnetic resonance imaging and step-section pathology evidence. Int J Radiat Oncol 2007;69:62–9.
[6] Lips IM, van der Heide UA, Haustermans K, van Lin EN, Pos F, Franken SP, et al. Single blind randomized Phase III trial to investigate the benefit of a focal lesion ablative microboost in prostate cancer (FLAME-trial): study protocol for a randomized controlled trial. Trials 2011;5:255.
[7] PIVOTALBoost [Internet]. NHS Health Research Authority. [cited 2019 Apr 24]. Available from: /planning-and-improving-research/application-summaries/research-summaries/pivotalboost/.
[8] Panebianco V, Giganti F, Kitzing YX, Cornud F, Campa R, De Rubeis G, et al. An update of pitfalls in prostate mpMRI: a practical approach through the lens of PI-RADS v. 2 guidelines. Insights Imaging 2018;9:87–101.
[9] Steenbergen P, Haustermans K, Lerut E, Oyen R, De Wever L, Van den Bergh L, et al. Prostate tumor delineation using multiparametric magnetic resonance imaging: inter-observer variability and pathology validation. Radiother Oncol 2015;115:186–90.
[10] Johnson DC, Raman SS, Mirak SA, Kwan L, Bajgiran AM, Hsu W, et al. Detection of individual prostate cancer foci via multiparametric magnetic resonance imaging. Eur Urol 2019;75:712–20.
[11] Silver DA, Pellicer I, Fair WR, Heston WD, Cordon-Cardo C. Prostate-specific membrane antigen expression in normal and malignant human tissues. Clin Cancer Res 1997;3:81–5.
[12] Fendler WP, Calais J, Eiber M, Flavell RR, Mishoe A, Feng FY, et al. Assessment of ^{68}Ga-PSMA-11 PET accuracy in localizing recurrent prostate cancer: a prospective single-arm clinical trial. JAMA Oncol 2019;28.
[13] Schmidt-Hegemann N-S, Stief C, Kim T-H, Eze C, Kirste S, Strouthos I, et al. Outcome after PSMA PET/CT-based salvage radiotherapy in patients with biochemical recurrence after radical prostatectomy: a 2-institution retrospective analysis. J Nucl Med 2019;60:227–33.
[14] Zamboglou C, Drendel V, Jilg CA, Rischke HC, Beck TI, Schultze-Seemann W, et al. Comparison of ^{68}Ga-HBED-CC PSMA-PET/CT and multiparametric MRI for gross tumour volume detection in patients with primary prostate cancer based on slice by slice comparison with histopathology. Theranostics 2017;7:228–37.
[15] Zamboglou C, Wieser G, Hennies S, Rempel I, Kirste S, Soschynski M, et al. MRI versus 68Ga-PSMA PET/CT for gross tumour volume delineation in radiation treatment planning of primary prostate cancer. Eur J Nucl Med Mol Imaging 2016;43:889–97.
[16] Weinreb JC, Barentsz JO, Choyke PL, Cornud F, Haider MA, Macura KJ, et al. PI-RADS prostate imaging – reporting and data system: 2015, version 2. Eur Urol 2016;69:16–40.
[17] Zamboglou C, Schiller F, Fechter T, Wieser G, Jilg CA, Chirindel A, et al. 68Ga-HBED-CC-PSMA PET/CT versus histopathology in primary localized prostate cancer: a voxel-wise comparison. Theranostics 2016;6:1619–28.
[18] Peters M, van Son MJ, Moerland MA, Kerkmeijer LGW, Eppinga WSC, Meijer RP, et al. MRI-guided ultrafocal HDR-brachytherapy for localised prostate cancer: median 4 year results of a feasibility study. Int J Radiat Oncol Biol Phys [Internet] 2019 [cited 2019 Apr 14]. Available from: https://www.redjournal.org/article/S0360-3016(19)30399-2/abstract.
[19] Maenhout M, Peters M, Moerland MA, Meijer RP, van den Bosch MAAJ, Frank SJ, et al. MRI guided focal HDR brachytherapy for localized prostate cancer: toxicity, biochemical outcome and quality of life. Radiother Oncol 2018;129:554–60.
[20] Eiber M, Weirich G, Holzapfel K, Souvatzoglou M, Haller B, Rauscher I, et al. Simultaneous 68 Ga-PSMA HBED-CC PET/MRI improves the localization of primary prostate cancer. Eur Urol 2016;70:829–36.
[21] Rhee H, Thomas P, Shepherd B, Greenslade S, Vela I, Russell PJ, et al. Prostate specific membrane antigen positron emission tomography may improve the diagnostic accuracy of multiparametric magnetic resonance imaging in localized prostate cancer as confirmed by whole mount histopathology. J Urol 2016;196:1261–7.
[22] Berger I, Annabattula C, Lewis J, Shetty DV, Kam J, Maclean F, et al. 68Ga-PSMA PET/CT vs. mpMRI for locoregional prostate cancer staging: correlation with final histopathology. Prostate Cancer Prostatic Dis 2018;21:204–11.
[23] Kesch C, Vinsensia M, Radtke JP, Schlemmer HP, Heller M, Ellert E, et al. Intra-individual comparison of 18 F-PSMA-1007 PET/CT, multi-parametric MRI, and radical prostatectomy specimens in patients with primary prostate cancer: a retrospective, proof-of-concept study. J Nucl Med 2017;58:1805–10.
[24] Chen M, Zhang Q, Zhang C, Zhao X, Marra G, Gao J, et al. Combination of 68 Ga-PSMA PET/CT and multiparameter MRI improves the detection of clinically significant prostate cancer: a lesion by lesion analysis. J Nucl Med 2018. jnumed.118.221010.
[25] Hicks RM, Simko JP, Westphalen AC, Nguyen HG, Greene KL, Zhang L, et al. Diagnostic accuracy of ^{68}Ga-PSMA-11 PET/MRI compared with multiparametric MRI in the detection of prostate cancer. Radiology 2018;289:730–7.
[26] van Schie MA, Dinh CV, vanHoudt PJ, Pos FJ, Heijmink SWTJP, Kerkmeijer LGW, et al. Contouring of prostate tumors on multiparametric MRI: evaluation of clinical delineations in a multicenter radiotherapy trial. Radiother Oncol 2018;128:321–6.
[27] Onjukka E, Uzan J, Baker C, Howard L, Nahum A, Syndikus I. Twenty fraction prostate radiotherapy with intra-prostatic boost: results of a pilot study. Clin Oncol 2017;29:6–14.
[28] Mannweiler S, Amersdorfer P, Trajanoski S, Terrett JA, King D, Mehes G. Heterogeneity of prostate-specific membrane antigen (PSMA) expression in prostate carcinoma with distant metastasis. Pathol Oncol Res 2009;15:167–72.
[29] Donato P, Roberts MJ, Morton A, Kyle S, Coughlin G, Esler R, et al. Improved specificity with 68Ga PSMA PET/CT to detect clinically significant lesions "invisible" on multiparametric MRI of the prostate: a single institution comparative analysis with radical prostatectomy histology. Eur J Nucl Med Mol Imaging 2019;46:20–30.
[30] D'Amico AV, Whittington R, Malkowicz SB, Schultz D, Blank K, Broderick GA, et al. Biochemical outcome after radical prostatectomy, external beam radiation therapy, or interstitial radiation therapy for clinically localized prostate cancer. JAMA 1998;280:6.
[31] Dearnaley D, Syndikus I, Mossop H, Khoo V, Birtle A, Bloomfield D, et al. Conventional versus hypofractionated high-dose intensity-modulated radiotherapy for prostate cancer: 5-year outcomes of the randomised, non-inferiority, phase 3 CHHiP trial. Lancet Oncol 2016;17:1047–60.
[32] Kishan AU, Cook RR, Ciezki JP, Ross AE, Pomerantz MM, Nguyen PL, et al. External beam radiotherapy, or external beam radiotherapy with brachytherapy boost and disease progression and mortality in patients with Gleason score 9–10 prostate cancer. JAMA 2018;319:896–905.
[33] Morris WJ, Tyldesley S, Rodda S, Halperin R, Pai H, McKenzie M, et al. Androgen Suppression Combined with Elective Nodal and Dose Escalated Radiation Therapy (the ASCENDE-RT Trial): an analysis of survival endpoints for a randomized trial comparing a low-dose-rate brachytherapy boost to a dose-escalated external beam boost for high- and intermediate-risk prostate cancer. Int J Radiat Oncol Biol Phys 2017;98:275–85.